Article

Dynamics of suspended and attached aerobic toluene degraders in small-scale flow-through sediment systems under growth and starvation conditions

Adrian Mellage, Dominik Eckert, Michael Grösbacher,
Ayse Zeynep Inan, Olaf Arie Cirpka, and Christian Griebler

Environ. Sci. Technol., **Just Accepted Manuscript** • DOI: 10.1021/es5058538 • Publication Date (Web): 26 May 2015

Dynamics of suspended and attached aerobic toluene degraders in small-scale flow-through sediment systems under growth and starvation conditions

Adrian Mellage,[†‡] Dominik Eckert,[†] Michael Grösbacher,[§] Ayse Z. Inan,[§] Olaf A. Cirpka, [†], Christian Griebler[§]*

† University of Tübingen, Center for Applied Geoscience, Hölderlinstrasse, 12, 72074 Tübingen, Germany

§ Helmholtz Zentrum München, Institute of Groundwater Ecology, Ingolstädter Landstrasse 1, 85764, Neuherberg, Germany

‡ now at: University of Waterloo, Department of Earth and Environmental Sciences, 200 University Ave. W, Waterloo, Ontario, Canada N2L 3G1

*Corresponding author

Phone: +49 7071 29 78928

Fax: +49 7071 29 5059

Email: olaf.cirpka@uni-tuebingen.de

Keywords: bio-reactive transport, flow-through system, biodegradation, natural attenuation.

ABSTRACT: The microbially mediated reactions, that are responsible for field-scale natural attenuation of organic pollutants, are governed by the concurrent presence of a degrading microbial community, suitable energy and carbon sources, electron acceptors, as well as nutrients. The temporal lack of one of these essential components for microbial activity, arising from transient environmental conditions, might potentially impair *in-situ* biodegradation. This study presents results of small scale flow-through experiments aimed at ascertaining the effects of substrate-starvation periods on the aerobic degradation of toluene by *Pseudomonas putida* F1. During the course of the experiments, concentrations of attached and mobile bacteria, as well as toluene and oxygen were monitored. Results from a fitted reactive-transport model, along with the observed profiles, show the ability of attached cells to survive substrate-starvation periods of up to four months and suggest a highly dynamic exchange between attached and mobile cells under growth conditions and negligible cell detachment under substrate-starvation conditions. Upon reinstatement of toluene, it was readily degraded without a significant lag period, even after a starvation period of 130 days. Our experimental and modeling results strongly suggest that aerobic biodegradation of BTEX-hydrocarbons at contaminated field sites is not hampered by intermittent starvation periods of up to four months.

INTRODUCTION

Natural and/or enhanced bioremediation has been identified as a non-invasive and cost-effective remediation strategy for aquifers contaminated with BTEX-hydrocarbons. The microbially mediated reactions, responsible for field-scale natural attenuation of these pollutants, are governed by their concentration distribution and subsequent availability of suitable energy-yielding electron acceptors[1]. Strong evidence exists that degradation reactions occur where mixing of electron donor and acceptor takes place[2-4].

Besides their intensively documented growth behavior, microbial populations in the subsurface undergo a variety of non-growth processes (i.e., transport as well as adaptive behaviors to cope with transient environmental conditions) that have the potential to affect contaminant degradation in the subsurface.

While microorganisms attached to the sediments have been found to comprise the largest portion of microbial biomass in the subsurface[5-7], studies on bioaugmentation and the spread of pathogens have shown that they partition between the sediments and the mobile aqueous phase and that they are transported in groundwater[8-14]. Only a limited number of studies, however, have considered the interdependent effects of microbial growth and transport[9, 15-18]. These studies observed that microbial growth, in addition to physical processes, strongly affects the partitioning of cells between the aqueous phase and the sediment surface. An increase in the number of suspended bacteria was observed after the addition of a growth substrate into the system[15-18]. However, the aforementioned studies did not monitor the response of biomass attached to the sediments throughout the experiments. Harvey et al.[19] observed that this increase in pore-water bacteria under growth conditions did not result in a reduction of attached cells.

Similar observations of lower ratios of attached to suspended cells in nutrient-rich zones have also been observed in laboratory[20] and field[21] studies.

Microbial populations are known to adapt to fluctuating environmental conditions[22]. In response to fluctuations, organisms may metabolically 'switch' into a so-called anabiotic state, referred to as dormancy[23]. Dormant cells do not exhibit behavioral patterns of living or dead cells, they merely enter a state of lowered metabolic activity in which they do not undergo cell division. Upon reinstatement of favorable conditions, they return to an 'alive' behavioral state[23], that is, the phenotypic shift from dormant to active is reversible[22]. Non-growth functions are maintained by consuming endogenous reserves[24-26].

Several studies have investigated the effects of unfavorable growth conditions on biodegradation[23, 25, 27-32]. Observations and modeling results show the resilience of degraders to stress and their ability to resume full metabolic functioning upon reinstatement of favorable conditions. Métris et al.[25] observed a degradation lag phase of a quarter of an hour after a three-day starvation period in a bioreactor system, exposed to changes in inlet concentrations of toluene and xylene. Matínez-Lavanchy et al.[32] observed no significant decline in biomass concentration during a period of oxygen deprivation of 12 h and observed increased growth of *Pseudomonas putida* and rapid toluene degradation upon the reinjection of an oxygen pulse into their experimental batch system. In batch experiments, Kaprelyants and Kell[31] observed that cells subjected to a starvation period of 75 days readily grew after 16 – 18 h of incubation in a system with a fresh substrate (lactate) containing medium.

In standard reactive-transport models, the degrading biota are assumed to be completely immobile, and their ability to adapt to unfavorable environmental conditions is not considered. The conventional dual-Monod modeling approach solely depends on the instantaneous

concentrations of reaction counterparts and does not account for degradation delays due to metabolic adaptations as well as concentration fluctuations[33-35]. A few studies attempted to incorporate the adaptive dormant behavior that microbial communities exhibit under unfavorable conditions[27-29]. Bradford et al.[36] suggest that there is currently "a need to study and predict microbial transport and survival throughout a range of environmentally relevant conditions in the laboratory scale".

In the present study, we introduce the results of a meticulously monitored small-scale flow-through sediment system, studying the effects of substrate-starvation periods on the degradation of toluene by the aerobic strain *Pseudomonas putida* F1. The build-up of cells in the sediment, the breakthrough of mobile cells at the outflow, as well as the consumption of toluene (electron donor) and oxygen were monitored. The attached degraders were subjected to toluene-starvation periods of up to 130 days in duration. Unlike earlier studies, presented above, the growth of degrading cells and contaminant degradation were monitored under flow-through conditions in natural sediments, a setup closer to natural conditions than well-mixed batch systems. We fitted a reactive-transport model - which takes the aforementioned patterns of microbial behavior into account - to the experimental data in order to quantify the response of the aerobic degraders to phases of toluene starvation of up to four months. The general question addressed by this study is to which extent *in-situ* biodegradation of contaminants is hampered by temporarily unfavorable conditions for the degrading microbial community, such as the temporal absence of growth substrates, which might, e.g., arise from a shift in contaminant plume position caused by changing hydraulic conditions.

EXPERIMENTAL SECTION

Experimental Setup. We performed experiments with the aerobic toluene degrader *Pseudomonas putida* F1 in small, cylindrical flow-through mini-columns (length: 1.60 cm; diameter: 1.34 cm). To follow the temporal evolution of attached cells throughout the experiments, we ran multiple mini-columns in parallel and dismantled replicate columns at specific time points. The mini-columns were packed with natural sediment of the middle sand fraction (200 – 630 μm). The measured effective porosity (n_e) in the mini-columns was 30%. Experiments were performed at a seepage velocity of 1.8 m d^{-1}. A multi-channel peristaltic pump (Ismatech, Wertheim, Germany) was used to achieve the desired flow rate. Flow in each of the mini-columns, was from the bottom to the top (Figure 1).

The mini-columns were inoculated with one pore volume containing 10^4 to 10^5 *P. putida* F1 cells mL^{-1}, a bacterial concentration encountered in natural groundwater. In addition to the "reactive" mini-columns, one "control" mini-column, which was not inoculated with *P. putida* F1, was run for each experiment. A bicarbonate-buffered freshwater medium was continuously infiltrated as mineral medium[37]. After inoculation, toluene was supplied at a concentration of approximately 6 mg L^{-1}. To prevent microbial growth in the inlet tubing, media containing toluene and oxygen (electron acceptor) were combined only at the injection to the mini-columns at a flow ratio of 1:9, respectively, from separate reservoirs.

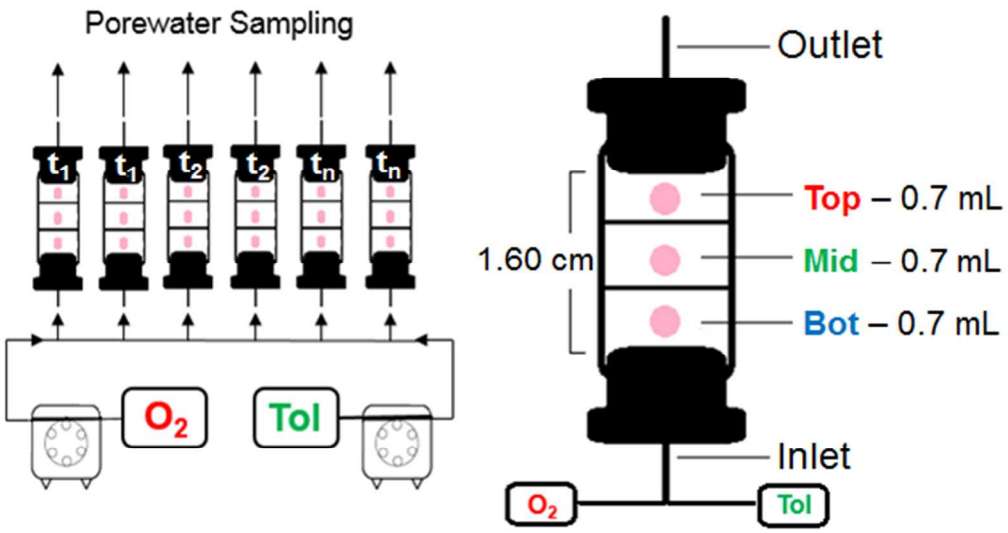

Figure 1. Schematic illustration of glass mini-columns used for all flow-through experiments.

For each mini-column three sections of equal dimensions, denoted bottom, middle and top, were assessed separately in terms of oxygen concentration, as well as attached bacterial cells. Each section contained a spot of oxygen sensitive foil (pink dots) for the monitoring of O_2 concentrations in the domain.

Water samples were collected at the inlet and outlet to monitor toluene degradation and transport of bacteria. Toluene concentrations were measured by GC-MS analysis[6], and cell numbers were quantified via flow cytometry[21]. Each experiment was run with a multitude of mini-columns in parallel. At specified time points, mini-column duplicates were dismantled to measure the bacterial abundance, activity (ATP)[38] and mean volume of cells in the sediment. The sediment was partitioned into the three sections mentioned above (bottom, middle, and top), and each sediment layer was separately analyzed for attached cells. Oxygen concentrations in the flow-through mini-columns were measured non-invasively via an optode technique[39] (Fibox, PreSens GmbH, Regensburg, Germany) – implementing spots of oxygen-sensitive foil glued to the inner column wall at three different positions (bottom, middle and top).

We used the experimental setup summarized above to run experiments under three different scenarios regarding availability of the growth substrate, toluene: (1) an experiment in which the toluene, and the electron acceptor oxygen, were continuously supplied (continuous injection); (2) an experiment where the injection of toluene was halted twice for periods of 8 and 21 days, respectively (short-term starvation), and (3) an experiment similar to the second one but with a much longer single toluene-starvation period of 130 days (long-term starvation). During the starvation periods, oxygenated mineral medium was continuously injected into the mini-columns.

Conceptual Model. Experimental results from flow-through experiments (presented herein), involving the aerobic degradation of toluene in porous media by *Pseudomonas putida* F1, showed evidence of microbial transport, attachment, increased cell mobility under growth conditions and the resilience of attached *P. putida F1* cells to a four-month toluene-starvation period. In order to capture the observed trends, we considered both mobile and immobile microbial cells and incorporated the transport of bacteria in our model, simulating a scenario in which bacteria are not evenly distributed across all grain surfaces. The model contains rate laws for the attachment of mobile cells to particle surfaces and the detachment of immobile cells into the aqueous phase. This aspect allowed for a more dynamic microbial population. Partitioning of cells specifically due to growth of attached cells was incorporated in the model. The ability of bacteria to enter a dormant state in the absence of toluene, and resume growth during toluene-rich conditions was introduced via the implementation of an active and an inactive fraction of attached bacteria. The following section presents the specific equations used for each of the simulated scenarios.

Governing Equations. The one-dimensional reactive-transport model developed to simulate the flow-through experiments considers three mobile species, namely toluene, oxygen and suspended bacteria, and two immobile species, namely active attached bacteria and inactive attached bacteria. One-dimensional transport of all mobile species was described by the advection-dispersion-reaction equation:

$$\frac{\partial C}{\partial t} = D\frac{\partial^2 C}{\partial x^2} - v\frac{\partial C}{\partial x} + r \quad (1)$$

where C is the aqueous concentration of the relevant mobile species [mg L^{-1}], D is the dispersion coefficient [m^2 d^{-1}], v is the seepage velocity [m d^{-1}], and r represents a reactive source/sink term [mg L^{-1} d^{-1}]. A discussion on the validity of 1-D transport is given in the supporting information, section S4.

Microbial growth was simulated by dual-Monod kinetics, describing the dependence of microbial growth on the simultaneous presence of toluene (carbon source and electron donor) and oxygen (electron acceptor). The microbial growth rate r_{growth} is then given by:

$$r_{growth} = \mu_{max} \cdot \frac{C_{Tol}}{C_{Tol} + K_{Tol}} \cdot \frac{C_{O_2}}{C_{O_2} + K_{O_2}} \cdot C_{Bio} \quad (2)$$

where μ_{max} [d^{-1}] is the maximum specific growth rate of the bacteria, C_{Tol}[mg L^{-1}] is the toluene concentration and C_{O_2}[mg L^{-1}] is the oxygen concentration, K_{Tol} [mg L^{-1}] and K_{O_2} [mg L^{-1}] are the Monod coefficients for toluene and oxygen, respectively, and C_{Bio} is the concentration of biomass. In the model, growth of attached (immobile), C_{Bio}^{im} [cells L_{sed}^{-1}], as well as suspended (mobile) biomass, C_{Bio}^{mob} [cells L^{-1}], is considered.

The experimental results indicated that the number of attached bacteria leveled off at a maximum density, i.e., that there was a maximum carrying capacity of the system for attached bacteria C_{Bio}^{max} [cells L_{sed}^{-1}]. It has been observed that some bacterial strains exhibit less

attachment to sediment surfaces when the concentration of cells in the sediment is high, a phenomenon known as blocking[8]. The concept and processes behind "blocking", resulting in a maximum attachment capacity in sediments, are dealt with in more detail in other works[40-42]. Once C_{Bio}^{max} was reached, in the experiment, attached bacteria continued to grow. All new-grown cells, however, were released to the aqueous phase and finally left the mini-column. This release of new-grown cells from the sediment surface to the mobile aqueous phase, which was observed in previous studies[13, 14, 40, 41], is also known as cell-division mediated transport[34] and was implemented in the model by the dynamic, growth-depended detachment rate, $r_{daughter}$ [cells L_{sed}^{-1} d^{-1}]:

$$r_{daughter} = r_{growth}^{im} \cdot \left(\frac{C_{Bio}^{im}}{C_{Bio}^{max}} \right) \quad (3)$$

in which r_{growth}^{im} [cells L_{sed}^{-1} d^{-1}] is the growth rate of the attached bacteria. The expression considers all attached cells whether they are actively degrading or dormant – more details on these growth-dependent distinctions are given below.

In order to account for adhesion of suspended bacteria to particle surfaces, as well as the possible mobilization of attached bacteria due to non-growth processes, first-order rate expressions for attachment r_{att} [cells L^{-1} d^{-1}] and detachment r_{det} [cells L_{sed}^{-1} d^{-1}] were incorporated into the model:

$$r_{att} = k_{att} \cdot C_{Bio}^{mob} \cdot \left(1 - \frac{C_{Bio}^{im}}{C_{Bio}^{max}} \right) \quad (4)$$

$$r_{det} = k_{det} \cdot C_{Bio}^{im} \quad (5)$$

in which k_{att} [d^{-1}] and k_{det} [d^{-1}] are the first-order rate coefficients for attachment and detachment, respectively. The term $\left(1 - C_{Bio}^{im}/C_{Bio}^{max}\right)$ was introduced to account for the carrying

capacity of the system for attached cells[42]. When the density of attached cells approaches C_{Bio}^{max}, the attachment rate approaches zero.

In order to implement microbial dormancy, we considered active, $C_{Bio}^{im/ac}$, and inactive, $C_{Bio}^{im/in}$, attached bacteria. Deactivation of active attached bacteria under unfavorable conditions, i.e., in the absence of toluene as the sole carbon and energy source, and reactivation of inactive bacteria, once toluene injection was resumed, were implemented as pseudo first-order kinetic processes[27] in the model:

$$r_{deac} = (1-\theta) \cdot k_{deac} \cdot C_{Bio}^{im/ac} \tag{6}$$

$$r_{reac} = \theta \cdot k_{reac} \cdot C_{Bio}^{im/in} \tag{7}$$

where k_{deac} [d^{-1}] and k_{reac} [d^{-1}] are the first-order rate coefficients for deactivation and reactivation, respectively, and θ [-] is a switch function describing the transition between the active and inactive state of attached bacteria. The switch function is modified from Stolpovsky et al.[27]:

$$\theta = \frac{1}{\exp\left(\frac{C_{Tol}^{thresh} - C_{Tol}}{0.1 \cdot C_{Tol}^{thresh}}\right) + 1} \tag{8}$$

in which C_{Tol}^{thresh}[mg L^{-1}] is the threshold toluene concentration for microbial growth. The switch-function θ determines whether conditions are favorable or unfavorable for bacterial growth. It can take on values between 0, denoting maximally unfavorable conditions, and 1, marking optimal conditions.

Combining all expressions gives rise to a model system in which microbes grow when both substrate and electron acceptor are present. Their growth may result in detachment which implies the presence of a mobile population of biomass. Like toluene and oxygen, the mobile biomass undergoes transport but it can adhere to particle surfaces along its flow path. Both attached and

suspended bacteria are able to grow, consuming toluene and oxygen. However, due to the short mean water residence time (minutes) compared to the considerably long generation time (hours), and the finding that 99% of the bacteria per volume porous medium were attached to the sediments (see Results & Discussion section), growth of mobile bacteria was found to be insignificant. The governing equations are summarized as follows:

$$\frac{dC_{Tol}}{dt} = D\frac{d^2C_{Tol}}{dx^2} - v\frac{dC_{Tol}}{dx} - \frac{1}{n_e}\cdot r_{growth}^{im/ac}\cdot\frac{1}{Y} - r_{growth}^{mob}\cdot\frac{1}{Y} \quad (9)$$

$$\frac{dC_{O_2}}{dt} = D\frac{d^2C_{O_2}}{dx^2} - v\frac{dC_{O_2}}{dx} - f_{O_2}\cdot\frac{1}{n_e}\cdot r_{growth}^{im/ac}\cdot\frac{1}{Y} - f_{O_2}\cdot r_{growth}^{mob}\cdot\frac{1}{Y} \quad (10)$$

$$\frac{dC_{Bio}^{im/ac}}{dt} = r_{growth}^{im/ac} - r_{daughter} + n_e\cdot r_{att} - r_{det} - r_{deac} + r_{reac} \quad (11)$$

$$\frac{dC_{Bio}^{mob}}{dt} = D\frac{d^2C_{Bio}^{mob}}{dx^2} - v\frac{dC_{Bio}^{mob}}{dx} + r_{growth}^{mob} + \frac{1}{n_e}\cdot r_{daughter} - r_{att} + \frac{1}{n_e}\cdot r_{det} \quad (12)$$

$$\frac{dC_{Bio}^{im/in}}{dt} = r_{deac} - r_{reac} \quad (13)$$

The rates of change of both toluene and oxygen concentrations depend on their consumption by the bacteria, which is proportional to microbial growth. The yield coefficient Y [cells mg_{sub}^{-1}] describes the amount of cells produced per mass of toluene degraded in the growth reactions and the stoichiometric coefficient f_{O_2} [mg_{ox}/mg_{tol}] relates the mass of oxygen consumed to the mass of toluene degraded. The effective porosity n_e is used as a conversion factor for unit agreement between the rates depending on the concentrations of attached bacteria and those of mobile bacteria.

Numerical Methods. The coupled system of five nonlinear partial differential equations was discretized in space by the cell-centered Finite Volume method ($\Delta x = 0.1$ mm), applying upwind differentiation of the advective term. The global implicit approach was adopted for the coupling of transport and reaction terms. The resulting system of nonlinear algebraic equations was linearized by the Newton-Raphson method. The code was written as a MATLAB program.

RESULTS & DISCUSSION

Experimental Results. Figure 2 depicts the experimental data along with the corresponding simulation results. The figure includes the results for the continuous injection experiment as well as the short- and long-term starvation experiments.

In the flow-through experiment with continuous toluene injection, steady-state conditions were reached after 1.5 to 2 days of experiment run-time – data points are illustrated in the left column of Figure 2. The marked drop in toluene concentrations is strongly mirrored by the oxygen consumption in the system. The temporal evolution of dissolved oxygen concentrations measured in the bottom, middle and top part of the mini-columns are almost identical, indicating that oxygen consumption, and hence microbial activity, was restricted to the bottom (inflow) section of the mini-columns under steady-state conditions. The number of attached cells increased by two orders of magnitude during the first three days and then leveled off at a maximum of about 2×10^8 cells per mL of sediment (mL_{sed}) in the bottom section of the domain and about 1×10^8 cells mL_{sed}^{-1} in the middle and top sections. The number of cells suspended in the outflowing pore water also increased by two orders of magnitude within the initial growth phase. Once the maximum number of attached cells was reached, the amount of cells continuously washed out was constant throughout the remainder of the experiment. The wash-out of about 2×10^6 cells mL^{-1} suggests that attached cells, even though their density in the

sediment stayed constant, were still replicating, releasing the daughter cells into the mobile aqueous phase.

Over the course of the experiment, 76 % of the new-grown cells were flushed out of the column. To estimate the distribution of bacteria between water and sediment, we compared the amount of cells attached to the sediment in the top part of the column (close to the outlet) and the amount of cells in the outflowing water under stable conditions. Even though the majority of new-grown cells were flushed out of the column over time, the vast majority of cells per volume of porous media (99%) was found to be attached to the sediment surface. In conjunction with the short mean water residence time of only 13 minutes and thus short travelling time of suspended cells through the sediment mini-columns, this finding strongly suggests that the contribution of new-grown cells stemming from suspended cells was negligible for our experiment.

The data points in the second and third columns of Figure 2 show the results of the short-term (middle column) and long-term starvation experiment (right column), respectively. In the short-term starvation experiment, the oxygen concentration in the column outlet rapidly dropped to effectively zero during the periods of toluene injection and initially rebounded to about 8 mg L^{-1} when toluene injection was stopped, but decreased to a level of about 6 mg L^{-1} for the remainder of the starvation periods. The maximum toluene concentrations detected after the resumption of toluene injection at the end of the two starvation phases was less than half of the injected concentration, and the concentration values declined to the level observed before the onset of starvation within hours. This indicates that the attached bacteria were able to degrade toluene right away, even after the absence of toluene for a period of three weeks during the second starvation phase.

The initial growth phase in the short-term starvation experiment (from day 1 to 4) resulted in the highest numbers of attached cells in the three experiments, with cell densities of about 1×10^9 cells mL_{sed}^{-1} in the bottom (inflow section) of the domain. While, the number of attached cells decreased to a level similar to the one observed in the other two experiments during the first starvation phase, the number of attached cells stayed constant during the second starvation phase. The breakthrough of suspended cells at the outflow showed evidence of periodic variations in conjunction with toluene-injection switches. The number of out-washed cells was highest during growth periods, reaching cell concentrations in the outflowing water similar to the ones detected in the continuous-injection experiment, and precipitously declined by around one order of magnitude during the starvation periods, followed by a swift increase to the previous level upon reinstatement of substrate injection.

The right column of Figure 2 shows the results for the long-term starvation experiment with a single starvation phase of four months. Trends are similar to those of the short-term starvation experiment. The number of attached cells increased by a factor of 15 during the first three days and stayed constant during the 130-day starvation period in the bottom (inflow) part of the column, while it decreased by approximately 30 and 70% in the mid and top part, respectively. The maximum observed density of attached cells was approximately 7.8×10^8 cells mL_{sed}^{-1} and thus about two times larger than in the continuous-injection experiment. Similar to the short-term starvation experiment, we observed a constant out-wash of about 2×10^5 cells mL^{-1} during the starvation phase. The detection of similar cell densities at the column inlet, stemming from a contamination of the oxic mineral medium (blue diamonds in Figure 2), indicated that these cells may not have been produced in the sediment columns, but originated from the injection media (for details see S2 in the supporting information). Our results indicate that, within four months of

toluene starvation, no substantial number of attached *P. putida* F1 cells were lost due to detachment or biomass decay and that the attached cells were able to regain their full toluene-degradation potential within less than a quarter of a day after toluene injection was resumed on day 133.

The continuous injection of about 2×10^5 cells mL^{-1} indicated unintended contamination with microbial cells in the injection media. While we do not know the nature and origin of these "contaminant" cells, we could rule out that these were *P. putida* F1 cells or any other toluene-degrading strain. In addition to the "reactive" mini-columns we ran control mini-columns, which were not inoculated with *P. putida* F1, but fed with the same inflow solution. In contrast to the "reactive" mini-columns neither toluene degradation nor oxygen consumption was observed in the "control" mini-columns. For more detailed information on the issue of cell contamination please refer to section S2 in the supporting information.

In addition to the measurement of cell numbers, Figure 3 shows ATP concentrations and the bio-volume of the attached cells recorded during the four month starvation period. The ATP measurements suggest a reduction in cell activity by 70 to 90% after the injection of toluene was ceased. The cell volume decreased by a factor of four during the four months of toluene starvation. We hypothesize that the reduction in cell volume is at least partially associated with a loss of biomass, which may be utilized to gain energy for cell maintenance. While the oxygen measurements suggest slight, but consistent, oxygen consumption throughout the two starvation phases of the short-term starvation experiment, the detected oxygen consumption during the long-term starvation experiment was not consistent.

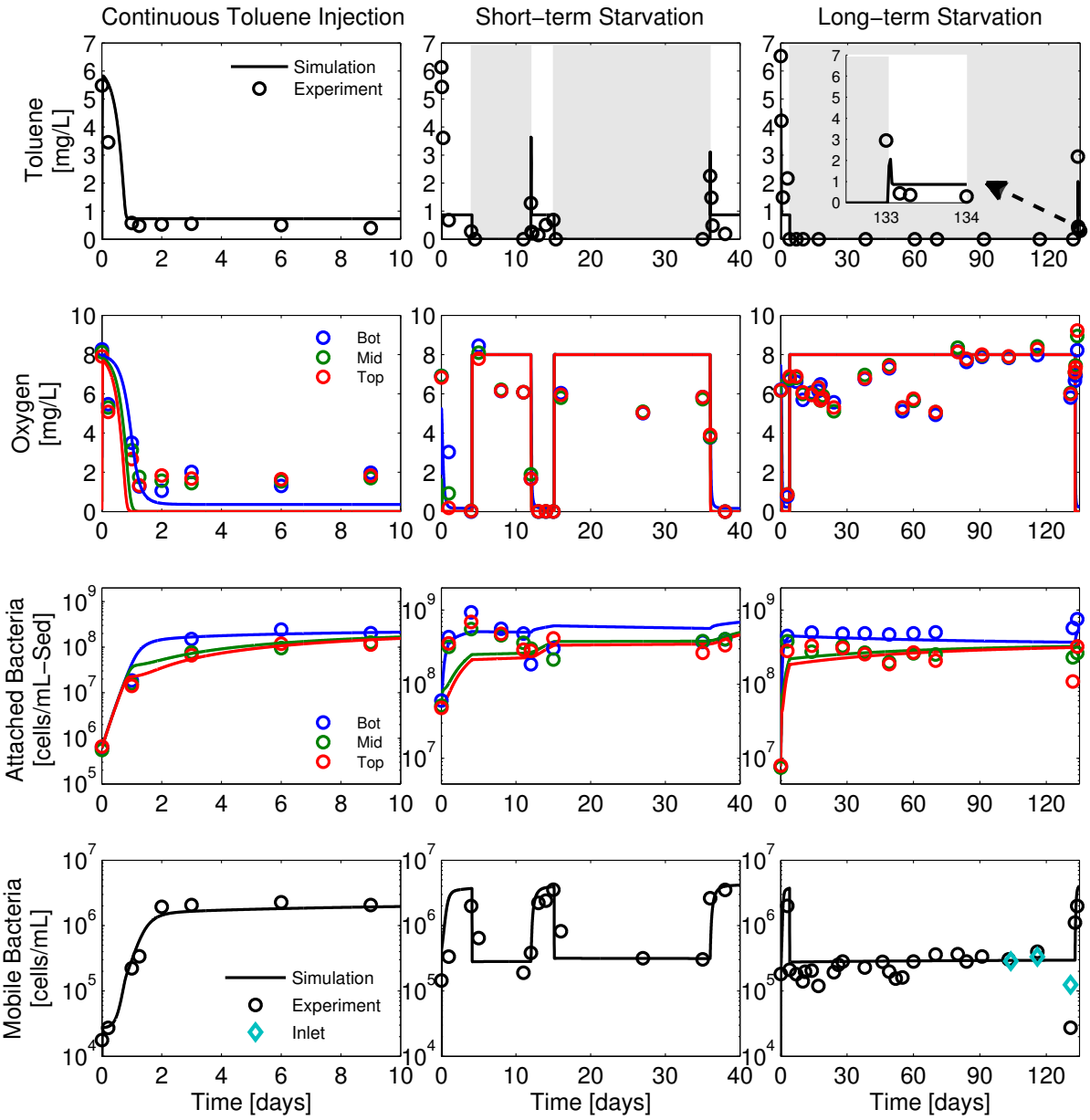

315

316 Figure 2. Experimental and simulation results for all three experimental setups (from left to
317 right): continuous toluene injections, short-term (8 days and 21 days) starvation and long-term
318 (130 days) starvation. The grey rectangles in the toluene plots in the upper row indicate the
319 toluene-starvation periods.

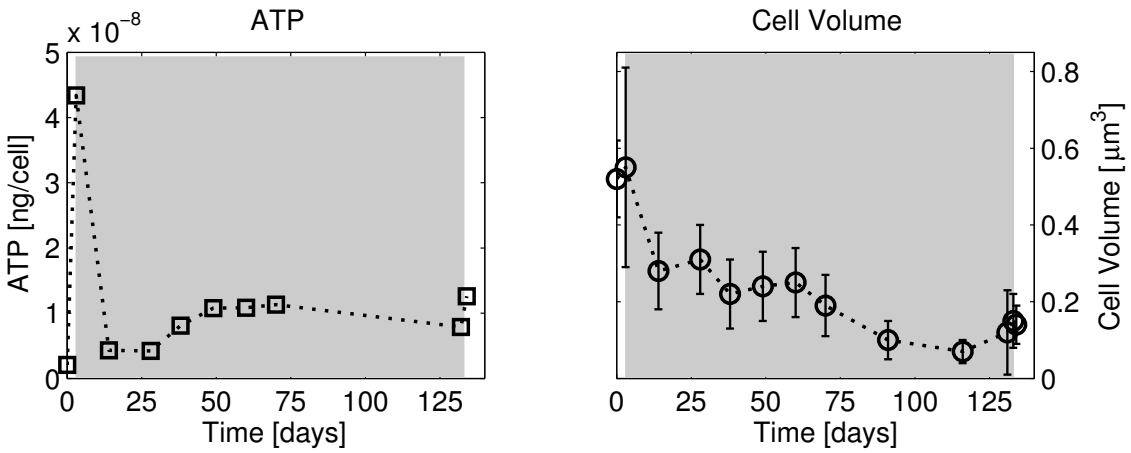

320

321 Figure 3. Change in the mass of ATP per cell over time in the bottom (inflow) part of the column
322 for the long-term starvation experiment (left subplot) and the temporal change of the cell bio-
323 volume of attached cells (right subplot). The area shaded in grey indicates the toluene-starvation
324 periods of 130 days.

325

326 **Simulation Results**. Figure 2 contains a comparison of the experimental data to the simulation
327 results of all three scenarios. The parameters of the reactive-transport model, applied to simulate
328 the column experiments, are summarized in Table 1. A discussion and justification of individual
329 parameter values is given in the supporting information, S1. The parameters in bold are fitted,
330 whereas all other parameters were determined prior to the reactive-transport simulations in batch
331 and flow-through experiments, or were taken from the literature. Except for slight variations in
332 the yield and the observed maximum amount of attached bacteria, the three experiments could be
333 adequately simulated using the same parameters. This effectively yielded a single model that
334 satisfactorily explained all experiments.

Table 1. Model parameters which best simulated the growth curves and concentration profiles observed in the experimental data. Parameters which were fitted to the data of the column experiments are given in bold. All remaining parameters were determined from batch and column experiments prior to the reactive-transport simulations or were taken from the literature.

Parameters		Continuous Injection	Short-term Starvation	Long-term Starvation	
μ_{max}	[d^{-1}]	4.5	4.5	4.5	batch
Y	[cells mg_{tol}^{-1}]	3.9×10^{8}	8.5×10^{8}	8.5×10^{8}	column[a]
K_{Tol}	[mg L^{-1}]	0.1	0.1	0.1	batch
K_{O_2} [43]	[mg L^{-1}]	0.32	0.32	0.32	literature
f_{O_2}	[mg_{ox} mg_{tol}^{-1}]	1.5	1.5	1.5	column[b]
C_{Bio}^{max}	[cells mL-PM^{-1}]	2.5×10^{8}	9.4×10^{8}	7.6×10^{8}	column[c]
$\boldsymbol{C_{Tol}^{thresh}}$	**[mg L^{-1}]**	**-**	**1×10^{-3}**	**1×10^{-3}**	**fitted**
$\boldsymbol{k_{att}}$	**[d^{-1}]**	**50**	**50**	**50**	**fitted**
$\boldsymbol{k_{det}}$	**[d^{-1}]**	**0.007**	**0.007**	**0.007**	**fitted**
$\boldsymbol{k_{deac}}$	**[d^{-1}]**	**-**	**2**	**2**	**fitted**
$\boldsymbol{k_{reac}}$	**[d^{-1}]**	**-**	**2**	**2**	**fitted**

[a]mass balance (new-grown cells/toluene degraded); [b]mass balance (oxygen consumed/toluene degraded); [c]maximum observed attached cell density

The simulation of the continuous-injection experiment yielded results in which the initial consumption of oxygen and toluene resulted in growth curves that closely fit measured attached cell concentrations during the initial growth phase. The parameterization of cell-division mediated transport, which simulated the expulsion of new-grown (daughter) cells from the

347 sediment surface to the mobile aqueous phase - once the carrying capacity of the system for
348 attached cells was reached - resulted in a simulated breakthrough of bacteria at the outflow
349 similar to the one observed. The measured oxygen concentrations plateaued at 1-2 mg L^{-1} under
350 stable conditions, while toluene could still be detected at the outflow. Oxygen profiles were not
351 accurately fitted to the measured profiles after the initial growth phase. Because the reaction is
352 highly energy yielding, it seems unlikely that oxygen values would all stabilize at such high
353 levels. Since the simulated oxygen profiles during the dynamic toluene injection experiments
354 follow similar trends as the data, the measured values for the continuous injection experiment
355 were treated with caution and the lack of a proper fit was attributed to a measurement bias -
356 caused by aging of the sensor foils, which were replaced in later experiments.
357 Results for the short-term starvation (middle column in Figure 2) simulation yielded oxygen
358 profiles that plateaued at values higher (about 2 mg L^{-1}) than the observed ones. This might
359 indicate that other pathways of oxygen consumption were at play in the mini-columns. A
360 possible explanation for this finding could be endogenous respiration of *P. putida* F1, the
361 oxidation of cell reserves in the absence of external substrates[26, 34]. The consumption of oxygen
362 in the absence of external energy sources has been observed in previous flow-through
363 experiments[18, 44]. The results of the oxygen measurements in the long-term starvation experiment
364 were not as conclusive as for the short-term starvation experiments. While most of the
365 measurements before day 70 of the experiment where about 2 mg L^{-1} lower than expected, the
366 measured concentrations for later times were similar to the inflow concentration.
367 While the model reproduced the concentrations of attached cells well for the continuous
368 injection experiment, experimental and simulation results showed some discrepancies for the two
369 starvation experiments. The model was not able to accurately reproduce the increased initial

growth spurt and subsequent decrease of cells attached to the sediment during the first starvation phase in the short-term starvation experiment. It was also not able to model the concentration of attached cells in the middle and bottom part of the column towards the end of the long-term starvation experiment.

The simulations of both the long-term (right column in Figure 2) and short-term starvation experiments were able to capture the abrupt drop in cell breakthrough during toluene-starvation conditions, pointing out the importance of considering peak cell detachment under growth conditions, which arises from the continuous proliferation of attached cells and the release of new-grown cells to the aqueous phase once the carrying capacity of the system for attached cells was reached. Cell detachment during the toluene-starvation phases was found to be negligible and the concentration of cells at the outflow during these periods was similar to the concentrations at the inflow. It cannot be ruled out that some of the imported cells from the supply medium replaced sediment cells that partitioned into the mobile phase. However, since the bacterial cells from the inflow did not contribute to toluene degradation, the fast recovery of full toluene degradation activity after the starvation period is clear evidence against the replacement of attached *P. putida* F1 cells by incomers - to a significant degree.

During the periods of toluene-starvation the bacteria enter a resting (inactive) state in which they survive by consuming cell reserves, this causes cells to decrease in size and also leads to a reallocation of resources which induces a change in cell elemental composition[24]. It is usually the case that biomass exposed to a new substrate needs to first initiate enzyme production and metabolic pathways and may need to repair cell damage, from the time of dormancy, before substrate consumption can begin, which is also known as metabolic lag[30]. The first-order activation rate coefficient determines the speed at which the bacteria are able to switch between

393 their inactive and active states. The fitted activation coefficient of 2 d^{-1} accurately modeled the
394 awakening period evident from the close fit of the peaks in toluene concentration at the outlet
395 upon reinjection.

396 The overall model fit and ability to reproduce the experimental system is good and its
397 performance is encouraging. The array of variables considered and measured depicts a complex
398 system. Discrepancies between model fit and experimental results are likely due to the transient
399 nature of natural processes and the fact that certain conditions can shift an organisms' response
400 to its environment. Such variability can lead to unexpected patterns, such as the initial growth
401 spurt in the short-term starvation experiment – not captured by the simulation. Information on
402 processes governing transience of model parameters was, however, not available. Therefore a
403 simplified approach was implemented.

404 IMPLICATIONS FOR IN-SITU BIODEGRADATION PROCESSES

405 In small-scale flow-through experiments performed with the aerobic toluene degrader *P.*
406 *putida* F1, we found that cells attached to the sediment matrix survived a toluene-starvation
407 period of four months. There was no significant loss in numbers of attached cells and the
408 attached cells regained their full biodegradation potential within a quarter of a day after toluene
409 reinjection into the system. Furthermore, the model-based analysis of the experimental data
410 showed the highly dynamic nature of microbial detachment. While detachment of *P. putida F1*
411 cells from the sediments was found to be negligible under toluene-starvation conditions, most of
412 the new-grown cells were released to the mobile water phase under growth conditions.

413 Our experimental and modeling results strongly suggest that in-situ biodegradation of toluene
414 at contaminated field sites is not hampered by periods of unfavorable (lack of substrate

availability) conditions. The temporal lack of toluene, which might arise from changes in contaminant plume position or variations in groundwater flow, will most likely not lead to a breakdown of the degradation capability of the microbial community if it has been established by exposure to the contaminants in the past, at least not under aerobic conditions.

So far, experiments were performed for toluene degradation under aerobic conditions. At many contaminated field sites, however, oxygen is only present at trace amounts, and contaminant degradation is governed by anaerobic processes[45, 46]. Towards this end, it is not clear if the results from the aerobic system can be directly transferred to biodegradation under anaerobic (e.g., sulfate reducing) conditions. Anaerobic conditions are energetically considerably less favorable than aerobic biodegradation - microbial growth and hence contaminant degradation rates are much smaller[47]. Similar arguments may hold for aerobic degradation of less energy-rich contaminants.

ACKNOWLEDGMENT

The authors acknowledge the support by the Deutsche Forschungsgemeinschaft under the grants Ci 26/9-1 and Gr 2107/3-1 as well as by the Helmholtz Association within the Helmholtz Water Center Munich.

ASSOCIATED CONTENT

Supporting Information. Additional material includes (S1) Model Parameters: a justification of individual parameter values. This material is available free of charge via the Internet at http://pubs.acs.org." The MATLAB code used in this study is available from the authors upon request.

AUTHOR INFORMATION

Corresponding Author

*Phone: +49-(0)7071-29-78928, Fax: +49-(0)7071-29-5059, E-mail: olaf.cirpka@uni-tuebingen.de

Author Contributions

M.G. performed the experimental work under the supervision of C.G.; A.M. and D.E. developed the model and fitted it to the data under the supervision of O.A.C.. All authors contributed to the writing of the paper.

Funding Sources

This research has been funded by Deutsche Forschungsgemeinschaft under the grants Ci 26/9-1 and Gr 2107/3-1 as well as by the Helmholtz Association within the Helmholtz Water Center Munich.

REFERENCES

1. Rees, H. C.; Oswald, S. E.; Banwart, S. A.; Pickup, R. W.; Lerner, D. N., Biodegradation processes in a laboratory-scale groundwater contaminant plume assessed by fluorescence imaging and microbial analysis. *Applied and Environmental Microbiology* **2007,** *73*, (12), 3865-3876.
2. Prommer, H.; Anneser, B.; Rolle, M.; Einsiedl, F.; Griebler, C., Biogeochemical and isotopic gradients in a BTEX/PAH contaminant plume: model-based interpretation of a high-resolution field data set. *Environmental Science & Technology* **2009,** *43*, (21), 8206-8212.
3. Thornton, S. F.; Quigley, S.; Spence, M. J.; Banwart, S. A.; Bottrell, S.; Lerner, D. N., Processes controlling the distribution and natural attenuation of dissolved phenolic compounds in a deep sandstone aquifer. *Journal of Contaminant Hydrology* **2001,** *53*, (3), 233-267.
4. Tuxen, N.; Albrechtsen, H.-J.; Bjerg, P. L., Identification of a reactive degradation zone at a landfill leachate plume fringe using high resolution sampling and incubation techniques. *Journal of Contaminant Hydrology* **2006,** *85*, (3), 179-194.
5. Griebler, C.; Mindl, B.; Slezak, D.; Geiger-Kaiser, M., Distribution patterns of attached and suspended bacteria in pristine and contaminated shallow aquifers studied with an in situ sediment exposure microcosm. *Aquatic Microbial Ecology* **2002,** *28*, (2), 117-129.

6. Anneser, B.; Einsiedl, F.; Meckenstock, R. U.; Richters, L.; Wisotzky, F.; Griebler, C., High-resolution monitoring of biogeochemical gradients in a tar oil-contaminated aquifer. *Applied Geochemistry* **2008,** *23*, (6), 1715-1730.
7. Alfreider, A.; Krössbacher, M.; Psenner, R., Groundwater samples do not reflect bacterial densities and activity in subsurface systems. *Water Research* **1997,** *31*, (4), 832-840.
8. Camesano, T. A.; Logan, B. E., Influence of fluid velocity and cell concentration on the transport of motile and nonmotile bacteria in porous media. *Environmental Science & Technology* **1998,** *32*, (11), 1699-1708.
9. Gargiulo, G.; Bradford, S.; Šimunek, J.; Ustohal, P.; Vereecken, H.; Klumpp, E., Transport and deposition of metabolically active and stationary phase *Deinococcus radiodurans* in unsaturated porous media. *Environmental Science & Technology* **2007,** *41*, (4), 1265-1271.
10. Haznedaroglu, B.; Kim, H.; Bradford, S.; Walker, S., Relative transport behavior of *Escherichia coli* O157: H7 and *Salmonella enterica* serovar pullorum in packed bed column systems: Influence of solution chemistry and cell concentration. *Environmental Science & Technology* **2009,** *43*, (6), 1838-1844.
11. Cunningham, A. B.; Sharp, R. R.; Caccavo Jr, F.; Gerlach, R., Effects of starvation on bacterial transport through porous media. *Advances in water resources* **2007,** *30*, (6), 1583-1592.
12. Redman, J. A.; Walker, S. L.; Elimelech, M., Bacterial adhesion and transport in porous media: Role of the secondary energy minimum. *Environmental Science & Technology* **2004,** *38*, (6), 1777-1785.
13. Chen, G.; Walker, S. L., Fecal indicator bacteria transport and deposition in saturated and unsaturated porous media. *Environmental Science & Technology* **2012,** *46*, (16), 8782-8790.
14. Stumpp, C.; Lawrence, J. R.; Hendry, M. J.; Maloszewski, P., Transport and bacterial interactions of three bacterial strains in saturated column experiments. *Environmental Science & Technology* **2011,** *45*, (6), 2116-2123.
15. Yolcubal, I.; Pierce, S. A.; Maier, R. M.; Brusseau, M. L., Biodegradation during Contaminant Transport in Porous Media. *Journal of Environmental Quality* **2002,** *31*, (6), 1824-1830.
16. Jordan, F. L.; Sandrin, S. K.; Frye, R. J.; Brusseau, M. L.; Maier, R. M., The influence of system complexity on bacterial transport in saturated porous media. *Journal of Contaminant Hydrology* **2004,** *74*, (1), 19-38.
17. Clement, T.; Peyton, B.; Skeen, R.; Jennings, D.; Petersen, J., Microbial growth and transport in porous media under denitrification conditions: experiments and simulations. *Journal of Contaminant Hydrology* **1997,** *24*, (3), 269-285.
18. Murphy, E. M.; Ginn, T. R.; Chilakapati, A.; Resch, C. T.; Phillips, J. L.; Wietsma, T. W.; Spadoni, C. M., The influence of physical heterogeneity on microbial degradation and distribution in porous media. *Water Resources Research* **1997,** *33*, (5), 1087-1103.
19. Harvey, R. W.; Smith, R. L.; George, L., Effect of organic contamination upon microbial distributions and heterotrophic uptake in a Cape Cod, Mass., aquifer. *Applied and Environmental Microbiology* **1984,** *48*, (6), 1197-1202.
20. Bengtsson, G., Growth and metabolic flexibility in groundwater bacteria. *Microbial Ecology* **1989,** *18*, (3), 235-248.
21. Anneser, B.; Pilloni, G.; Bayer, A.; Lueders, T.; Griebler, C.; Einsiedl, F.; Richters, L., High resolution analysis of contaminated aquifer sediments and groundwater—what can be learned in terms of natural attenuation? *Geomicrobiology Journal* **2010,** *27*, (2), 130-142.

510 22. Kussell, E.; Kishony, R.; Balaban, N. Q.; Leibler, S., Bacterial persistence a model of
511 survival in changing environments. *Genetics* **2005,** *169*, (4), 1807-1814.
512 23. Kaprelyants, A. S.; Gottschal, J. C.; Kell, D. B., Dormancy in non-sporulating bacteria.
513 *FEMS Microbiology Letters* **1993,** *104*, (3-4), 271-286.
514 24. Lennon, J. T.; Jones, S. E., Microbial seed banks: the ecological and evolutionary
515 implications of dormancy. *Nature Reviews Microbiology* **2011,** *9*, (2), 119-130.
516 25. Métris, A.; Gerrard, A. M.; Cumming, R. H.; Weigner, P.; Paca, J., Modelling shock
517 loadings and starvation in the biofiltration of toluene and xylene. *Journal of Chemical*
518 *Technology and Biotechnology* **2001,** *76*, (6), 565-572.
519 26. Mason, C.; Hamer, G.; Bryers, J., The death and lysis of microorganisms in
520 environmental processes. *FEMS microbiology letters* **1986,** *39*, (4), 373-401.
521 27. Stolpovsky, K.; Martinez-Lavanchy, P.; Heipieper, H. J.; Van Cappellen, P.; Thullner,
522 M., Incorporating dormancy in dynamic microbial community models. *Ecological Modelling*
523 **2011,** *222*, (17), 3092-3102.
524 28. Bär, M.; Hardenberg, J.; Meron, E.; Provenzale, A., Modelling the survival of bacteria in
525 drylands: the advantage of being dormant. *Proceedings of the Royal Society of London. Series B:*
526 *Biological Sciences* **2002,** *269*, (1494), 937-942.
527 29. Wirtz, K. W., Control of biogeochemical cycling by mobility and metabolic strategies of
528 microbes in the sediments: an integrated model study. *FEMS Microbiology Ecology* **2003,** *46*,
529 (3), 295-306.
530 30. Wood, B. D.; Ginn, T. R.; Dawson, C. N., Effects of microbial metabolic lag in
531 contaminant transport and biodegradation modeling. *Water Resources Research* **1995,** *31*, (3),
532 553-563.
533 31. Kaprelyants, A. S.; Kell, D. B., Dormancy in stationary-phase cultures of Micrococcus
534 luteus: flow cytometric analysis of starvation and resuscitation. *Applied and Environmental*
535 *Microbiology* **1993,** *59*, (10), 3187-3196.
536 32. Martínez-Lavanchy, P. M.; Müller, C.; Nijenhuis, I.; Kappelmeyer, U.; Buffing, M.;
537 McPherson, K.; Heipieper, H. J., High stability and fast recovery of expression of the TOL
538 plasmid-carried toluene catabolism genes of Pseudomonas putida mt-2 under conditions of
539 oxygen limitation and oscillation. *Applied and Environmental Microbiology* **2010,** *76*, (20),
540 6715-6723.
541 33. Bauer, R. D.; Maloszewski, P.; Zhang, Y.; Meckenstock, R. U.; Griebler, C., Mixing-
542 controlled biodegradation in a toluene plume—results from two-dimensional laboratory
543 experiments. *Journal of Contaminant Hydrology* **2008,** *96*, (1), 150-168.
544 34. Murphy, E. M.; Ginn, T. R., Modeling microbial processes in porous media.
545 *Hydrogeology Journal* **2000,** *8*, (1), 142-158.
546 35. Barry, D. A.; Prommer, H.; Miller, C. T.; Engesgaard, P.; Brun, A.; Zheng, C., Modelling
547 the fate of oxidisable organic contaminants in groundwater. *Advances in Water Resources* **2002,**
548 *25*, (8-12), 945-983.
549 36. Bradford, S. A.; Wang, Y.; Kim, H.; Torkzaban, S.; Šimůnek, J., Modeling
550 Microorganism Transport and Survival in the Subsurface. *Journal of Environmental Quality*
551 **2014,** *43*, (2), 421-440.
552 37. Widdel, F.; Bak, F., Gram-negative mesophilic sulfate-reducing bacteria. In *The*
553 *Prokaryotes*, Springer: 1992; pp 3352-3378.

554 38. Hammes, F.; Goldschmidt, F.; Vital, M.; Wang, Y.; Egli, T., Measurement and
555 interpretation of microbial adenosine tri-phosphate (ATP) in aquatic environments. *Water*
556 *Research* **2010,** *44*, (13), 3915-3923.
557 39. Haberer, C. M.; Rolle, M.; Liu, S.; Cirpka, O. A.; Grathwohl, P., A high-resolution non-
558 invasive approach to quantify oxygen transport across the capillary fringe and within the
559 underlying groundwater. *Journal of Contaminant Hydrology* **2011,** *122*, (1), 26-39.
560 40. Tan, Y.; Gannon, J.; Baveye, P.; Alexander, M., Transport of bacteria in an aquifer sand:
561 Experiments and model simulations. *Water Resources Research* **1994,** *30*, (12), 3243-3252.
562 41. Bolster, C. H.; Mills, A. L.; Hornberger, G. M.; Herman, J. S., Effect of surface coatings,
563 grain size, and ionic strength on the maximum attainable coverage of bacteria on sand surfaces.
564 *Journal of Contaminant Hydrology* **2001,** *50*, (3), 287-305.
565 42. Ding, D., Transport of bacteria in aquifer sediment: experiments and modeling.
566 *Hydrogeology journal* **2010,** *18*, (3), 669-679.
567 43. Bauer, R. D.; Rolle, M.; Bauer, S.; Eberhardt, C.; Grathwohl, P.; Kolditz, O.;
568 Meckenstock, R. U.; Griebler, C., Enhanced biodegradation by hydraulic heterogeneities in
569 petroleum hydrocarbon plumes. *Journal of Contaminant Hydrology* **2009,** *105*, (1), 56-68.
570 44. Eckert, D. K., P.; Bauer, R.; Griebler, C.; Cirpka, O. A., Fringe-controlled biodegradation
571 under dynamic conditions: Quasi 2-D flow-through experiments and reactive-transport modeling.
572 *Journal of Contaminant Hydrology* **in press**.
573 45. Lovley, D. R., Bioremediation - Anaerobes to the rescue. *Science* **2001,** *293*, (5534),
574 1444-1446.
575 46. Wiedemeier, T. H.; Rifai, H. S.; Newell, C. J.; Wilson, J. T., *Natural Attenuation of Fuels*
576 *and Chlorinated Solvents in the Subsurface*. John Wiley and Sons Inc.: 1999.
577 47. Rittmann, B. E.; McCarty, P. L., *Environmental biotechnology: principles and*
578 *applications*. Tata McGraw-Hill Education: 2012.

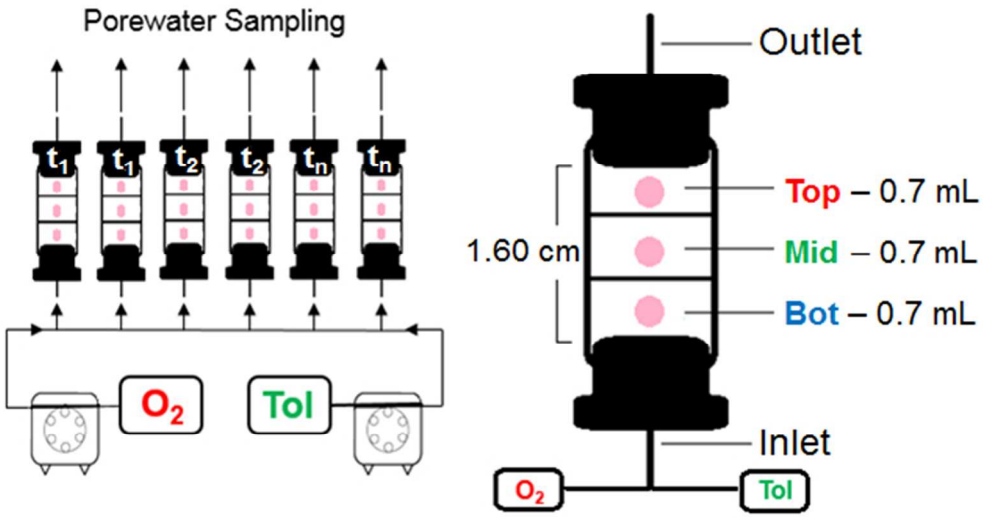

Schematic illustration of glass mini-columns used for all flow-through experiments.
169x91mm (96 x 96 DPI)

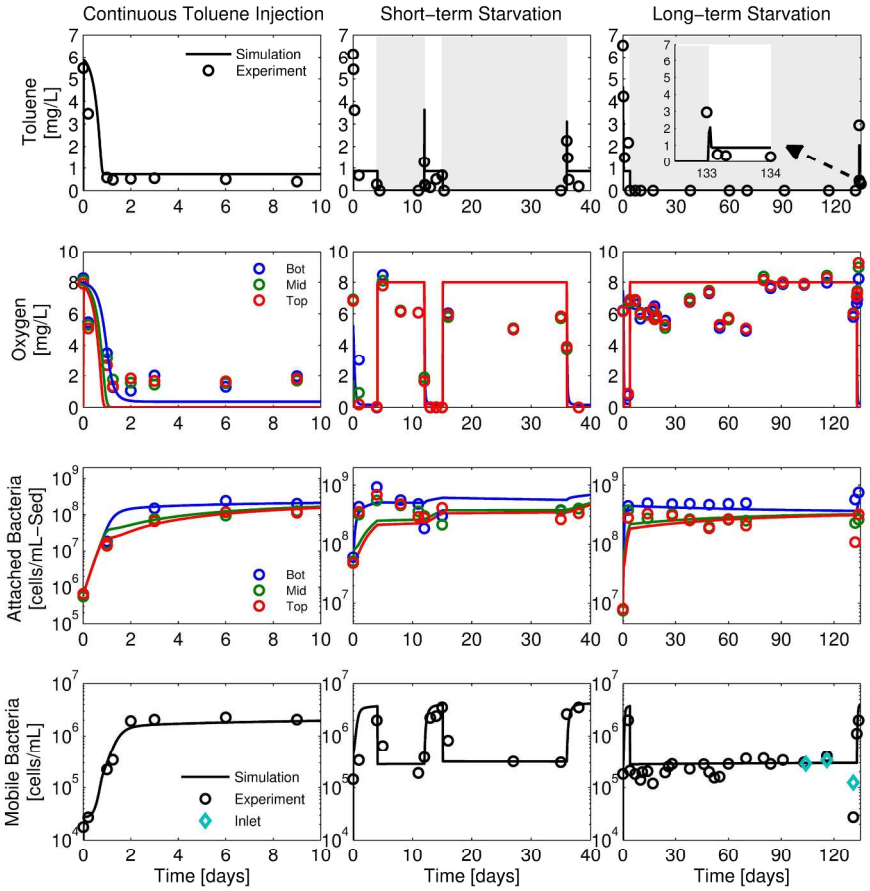

Experimental and simulation results for all three experimental setups (from left to right): continuous toluene injections, short-term (8 days and 21 days) starvation and long-term (130 days) starvation. The grey rectangles in the toluene plots in the upper row indicate the toluene-starvation periods.
224x221mm (300 x 300 DPI)

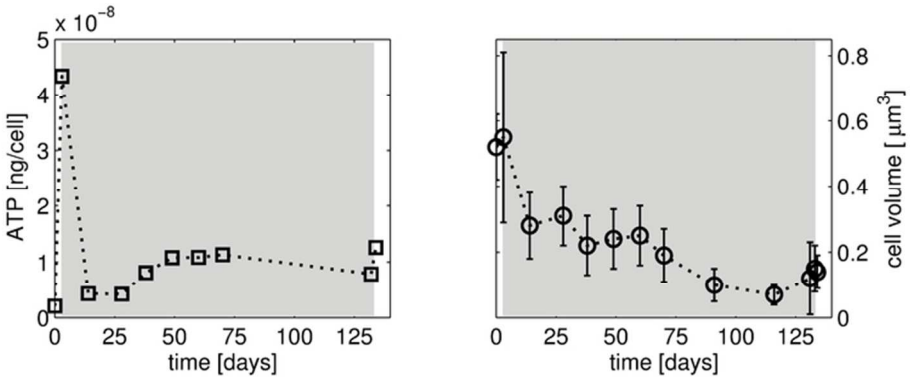

Change in the mass of ATP per cell over time in the bottom (inflow) part of the column for the long-term starvation experiment (left subplot) and the temporal change of the cell bio-volume of attached cells (right subplot). The area shaded in grey indicates the toluene-starvation periods of 130 days.
69x26mm (300 x 300 DPI)

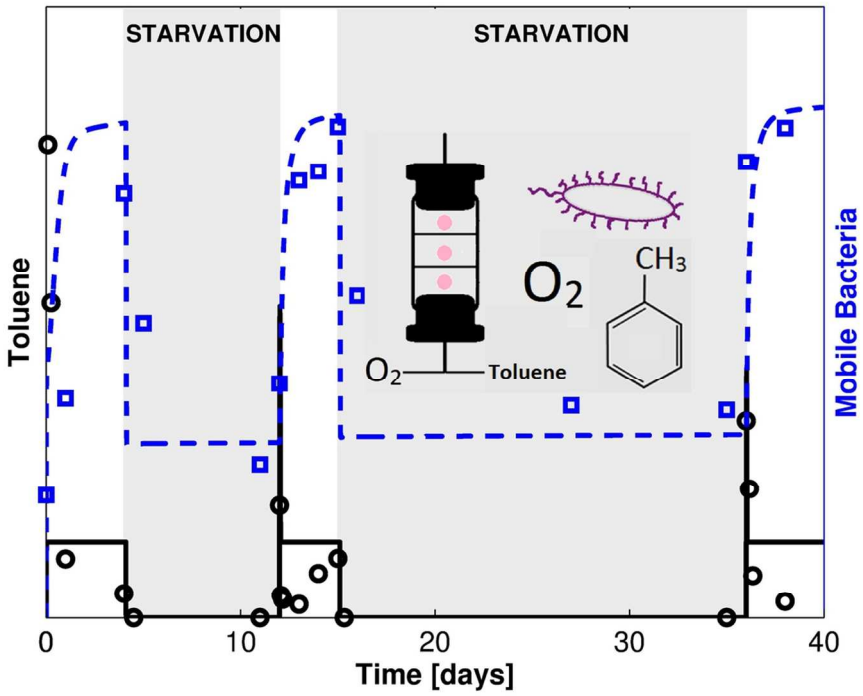

111x83mm (300 x 300 DPI)